PCCP

Accepted Manuscript

ROYAL SOCIETY OF CHEMISTRY

www.rsc.org/pccp

Journal Name

RSCPublishing

ARTICLE

β-Phenyl Quenching of 9-Phenylphenalenone. A novel Photocyclisation Reaction with Biological Implications

Cite this: DOI: 10.1039/xoxxoooooox

Received ooth January 2012,
Accepted ooth January 2012

DOI: 10.1039/xoxxoooooox

www.rsc.org/

Götz Bucher,[a] Roger Bresolí-Obach,[b] Carme Brosa,[b] Cristina Flors,[b,c] Javier G. Luis,[d,e] Teresa A. Grillo,[d,e] and Santi Nonell[b*]*

The singlet and triplet excited states of 9-phenylphenalenones **1** undergo β-phenyl quenching (BPQ) via addition of the carbonyl oxygen to the *ortho* position of the phenyl substituent. This reaction leads to the formation of naphthoxanthenes **4**, which, in the absence of quenchers, undergo a very rapid electrocyclic ring opening reaction reverting to **1** within a few microseconds. Naphthoxanthene **4a** contains a remarkably weak C-H bond, which enables efficient hydrogen transfer reactions to suitable acceptors, giving rise to the production of the naphthoxanthenyl radical or the naphthoxanthenium cation, depending on the solvent polarity. The study uncovers a number of new aspects of BPQ and suggests an excited state-mediated metabolic pathway in the biosynthesis of plant fluorones.

1. Introduction

9-Phenylphenalenones **1** (Scheme 1) are natural products produced by banana plants (e.g., *Musa acuminata*) upon infection with the fungus *Mycosphaerella fijiensis*.[1–3] Our interest in these compounds stems from the fact that phenalenone is well known for its high efficiency in photosensitising the production of singlet molecular oxygen ($O_2(a^1\Delta_g)$ or $^1O_2$).[4–6] Thus, 9-phenylphenalenones are phototoxic for a variety of microorganisms and we established that $^1O_2$ is involved in the process,[1,2] which led us to propose that light-induced processes participate in the defence mechanism of the infected plants.[2] Intriguingly, while phenalenone produces $^1O_2$ with quantum yield close to unity, yields in 9-phenylphenalenones are an order of magnitude smaller.[1,2]

In a previous communication, attempts were made to rationalise this observation, which revealed the formation of transient species in competition with $^1O_2$ production.[7] The exact nature of the competing processes remains however unknown, although it was shown that they might involve a charge-transfer component. Recent work aimed at producing naphthoxanthenyl, a remarkable stable radical, led us to propose that the transient species could in fact be a 1*H*-2-6a*H*-naphtho[2,1,8-mna]xanthene (hereafter naphthoxanthene),[8] that could be formed in a formal 6-π electrocyclic intramolecular photocyclisation of **1** through the β-phenyl quenching (BPQ) mechanism.[9–17]

In this contribution, we report a comprehensive theoretical and experimental investigation of the role of BPQ in the photochemistry of **1**. The new results confirm the production of naphthoxanthenes and uncover their reactivity. From a fundamental point of view, the rigidity of 9-phenylphenalenones provides a unique framework for extending the current knowledge on BPQ of aromatic ketones and expands the scope of its applications. In addition, our observations contribute to the understanding the participation of light in natural product metabolic pathways.

2. Results and discussion

2.1 Potential pathways for BPQ of 9-phenylphenalenones.

In BPQ, the excited states of aryl ketones bearing a phenyl ring in β-position, such as β-phenylpropiophenone, are quenched very efficiently by an intramolecular reaction. It has been recently shown that the mechanism of BPQ involves addition of the carbonyl oxygen atom of the triplet excited ketone to the *ipso*- or *ortho*-positions of the β-phenyl ring, followed by ISC of the biradical formed.[18] On

the singlet spin manifold, the biradicals are no minima on the potential energy hypersurface and relax to the singlet ground states of the ketone.

We thus investigated computationally possible pathways for BPQ in 9-phenylphenalenones. As in the case of β-phenylpropiophenone, BPQ in ^{3}**1***, and possibly also in ^{1}**1*,** could occur via addition of the carbonyl oxygen atom to either the *ipso*- or *ortho* position of the 9-phenyl substituent (Scheme 2).

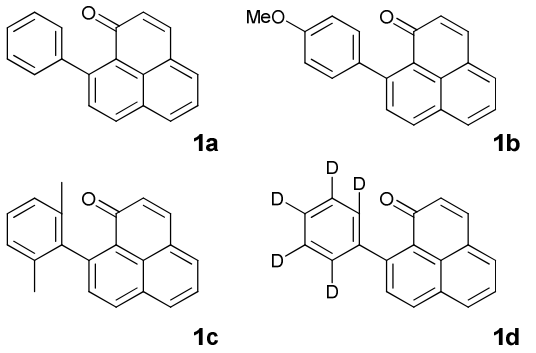

Scheme 1: 9-Phenylphenalenones studied in this work. See the ESI for a comprehensive list of naturally-occurring derivatives of **1a**.

Scheme 2 shows calculated energy of the corresponding BPQ intermediates, transition states and products for three derivatives of **1** (**1a**: R = R' = H, **1b**: R = OCH_3, R' = H, **1c**: R = H, R' = CH_3) obtained using two different computational approaches ((U)B3LYP/cc-pVTZ//(U)B3LYP/6-31G(d), and (U)B3PW91/cc-pVTZ//(U)B3PW91/6-31G(d)). As in a previous work,[18] the different DFT methods yield results that are in qualitative agreement with each other. For simplicity, we have restricted our calculations to BPQ from the triplet state and have also ruled out any significant contribution from the upper-lying (n,π*) triplet state.

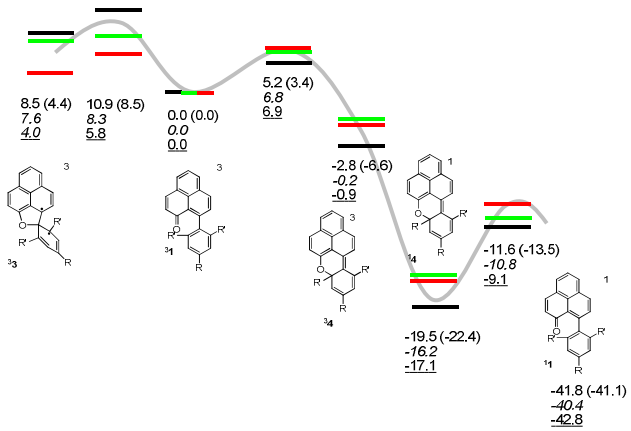

Scheme 2: Reaction pathways after triplet excitation of **1a-c**. Enthalpies are given in kcal mol^{-1} relative to the triplet state. Without brackets: (U)B3LYP/cc-pVTZ//(U)B3LYP/6-31G(d). In brackets: (U)B3PW91/cc-pVTZ//(U)B3PW91/6-31G(d). In ordinary font / black bar: **1a** (R = H). In italics / green bar: **1b** (R = OCH_3). Underlined / red bar: **1c** (R' = CH_3). A solid line connecting the different states is provided as a visual aid only.

Unlike in the case of BPQ of β-phenylpropiophenone, addition to the *ortho*-position is predicted for **1a*** and **1b*** to be more favourable than to the *ipso* position. For **1c*** the *ortho*-activating influence of the two methyl groups significantly facilitates *ipso*-addition from the kinetics point of view, although thermodynamics still favours the *ortho* attack. Another difference to β-phenylpropiophenone lies in the fact that *ortho*-addition followed by ISC yields a minimum structure on the potential energy hypersurface. Thus our calculations predict that BPQ of **1a-c*** should yield closed-shell naphthoxanthenes **4a-c**.

The reaction coordinates leading from ^{3}**1a*** to the *ortho*-(^{3}**4a***) and *ipso*- (^{3}**3a***) addition products were further investigated by calculating intrinsic reaction coordinates (IRC). The IRC calculations were performed at the UB3LYP/6-31G(d) level of theory, followed by UB3LYP/cc-pVTZ single point energy calculations for every intermediary point along the IRCs on both the triplet and singlet (ground-state) spin manifolds. The C-O distances between the carbonyl oxygen atom and the *ipso*- or *ortho*-carbon atoms of the phenyl ring were taken as measure of the reaction coordinates, as they change monotonically along the reaction coordinates. Figure 1A shows the triplet and singlet energies. It clearly shows that the energy gap between singlet and triplet hypersurface is significantly reduced when moving along the reaction coordinates for both *ipso*- and *ortho*-attack in ^{3}**1a***. The small gap in the *ortho* product ^{3}**4a*** suggests rapid ISC to yield the ground-state singlet species **4a**. It is noted that the singlet wavefunctions retain closed-shell character ($S^2 = 0$) for much of the reaction coordinate of *ortho*-attack. A plot of S^2 vs. the C-O distance is given as Figure S1 (see Electronic Supplementary Information). In the case of the triplet biradical ^{3}**3a** formed by the far less favourable *ipso*-attack, the triplet state is predicted to be the ground state (See Scheme 2).

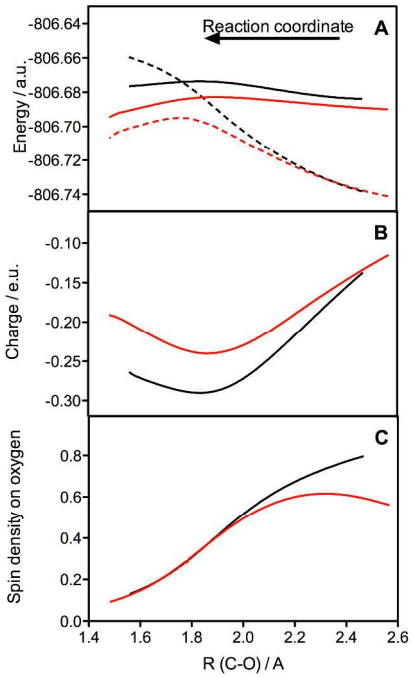

Figure 1: Intrinsic reaction coordinates leading from ^{3}**1a*** to the *ortho*- (^{3}**4a***) and *ipso*- (^{3}**3a***) addition products. The transition state is indicated by the data points at R ~ 1.85 Å (*ipso*) or 1.92 Å (*ortho*) **A**: Energy (in atomic units) vs. the O (carbonyl) – C (*ortho / ipso*) distance. Red: triplet energy, IRC for *ortho* attack. Dashed red: singlet energy at triplet geometry, IRC for *ortho* attack. Black: triplet energy, IRC for *ipso* attack. Dashed black: singlet energy at triplet geometry, IRC for *ipso* attack. Short C-O distances refer to products ^{3}**3a***/^{3}**4a*** (triplets) or **1a/4a** (ground-state singlets); long C-O distances to the ketones ^{3}**1a*** (triplet) or **1a** (ground-state singlet). **B**: Negative charge on the phenalenone moiety in ^{3}**1a***vs. the O (carbonyl) – C (*ortho / ipso*) distance. Red line: *ortho*-attack. Black line: *ipso*-attack. **C**: Spin density at the carbonyl oxygen atom of ^{3}**1a*** *vs.* the O-C$_{(ipso/ortho)}$ distance. Red line: *ipso*-attack. Black line: *ortho*-attack.

Figure 1B shows the degree of charge transfer to the phenalenone moiety along the reaction coordinate. As in BPQ of derivatives of β-phenylpropiophenone having a (π,π*) lowest triplet excited state, charge transfer to the ketone moiety is much more pronounced in case of the *ipso*-attack,[18] consistent with the (π,π*) configuration of ^{3}**1a-c***.

Finally, Figure 1C shows a plot of the spin density at the oxygen atom vs. the C-O distance and clearly reveals that spin density exceeding that of ^{3}**1a*** in its equilibrium geometry (calculated as 0.51 at the same level of theory) has to be localized at the oxygen atom for the addition reaction to occur. In case of the *ortho*-attack, the spin density at oxygen initially rises to a maximum and then falls again, whereas in case of *ipso*-attack, the oxygen spin density falls steadily. A possible interpretation of this finding would be that *ortho*-attack occurs from the (π,π*) lowest triplet excited state of **1a**, whereas *ipso*-attack would require population of the higher-lying (n,π*) triplet state.

The energy calculations finally indicate also that the ground-state BPQ products, ^{3}**3** and **4**, are less stable than ground-state **1** and are therefore predicted to revert to **1** by electrocyclic ring opening. The activation enthalpy for this process is calculated (B3LYP) as $\Delta H^{\ddagger}$ = 7.9, 5.4, and 5.4 kcal mol^{-1} for **4a-c**, respectively. Using B3PW91 the value $\Delta H^{\ddagger}$ = 8.9 kcal mol^{-1} is obtained for **4a,** in fairly good agreement. The results compare favourably with experimental values (8.9 and 7.2 kcal·mol^{-1} for **4a** and **4b**, respectively).[7] Figure 2 shows optimized structures of stationary points relevant to BPQ of ^{3}**1a** and for the decay of its photoproduct **4a**.

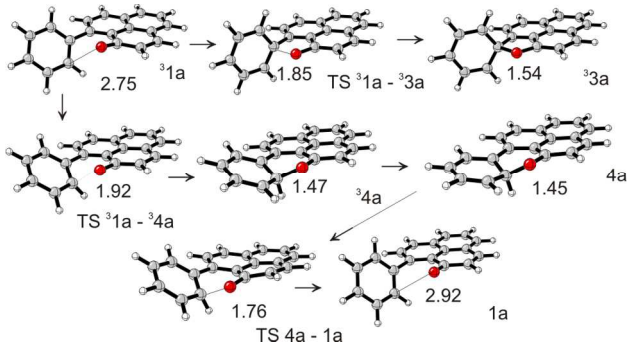

Figure 2: Optimized geometries ((U)B3LYP/6-31G(d)) of stationary points relevant to BPQ of **1a**. The numbers indicate important distances between the oxygen atom and the *ortho*- or *ipso* carbon atoms of the phenyl substituent (in Å).

2.2 Characterization of BPQ products

Evidence for the proposed BPQ pathways was derived from spectroscopic measurements. Photolysis (diode, λ = 395 nm, 20 min) of **1a**, matrix-isolated in Ar at T = 10 K, led to the formation of a red matrix with new UV-Vis bands at λ_{max} = 501 nm and λ = 290 nm (Figure 3). The spectrum is similar to that observed at room temperature by transient absorption, λ_{max} = 520 nm,[7] and is consistent with the calculated UV-Vis spectrum of **4**a (B3LYP/6-31G(d)), which shows maxima at 345 and 565 nm (Figure 3, inset).

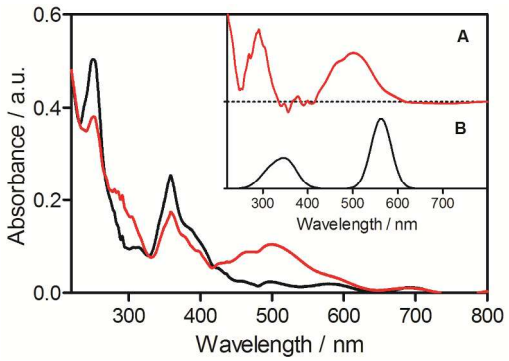

Figure 3: UV/Vis spectrum of **1a**, matrix-isolated in Ar at T = 10 K, before (black) and after (red) photolysis (diode, λ = 395 nm, 20 min). Inset: **A:** Difference absorption spectrum. **B**: Calculated spectrum of naphthoxanthene **4a**.

Under all photolytic conditions tested, conversion to **4a** was partial only, indicating the presence of a photostationary equilibrium between **1a** and **4a**. Subsequent photolysis

(diode, λ = 530 nm, 20 min) resulted in the complete disappearance of the new bands, and to the reversion of the matrix colour to yellow. The difference IR spectrum of the matrix before and after the secondary photolysis at 530 nm is shown in Figure 4. There is an excellent match with the calculated difference spectrum (B3LYP/6-31G(d), scaled by 0.9614[19]) of **1a** and **4a**, and also with that found by step-scan transient IR experiments at room temperature (predicted: 1499 and 1321 cm^{-1}; observed: 1510 and 1310 cm^{-1})[7].

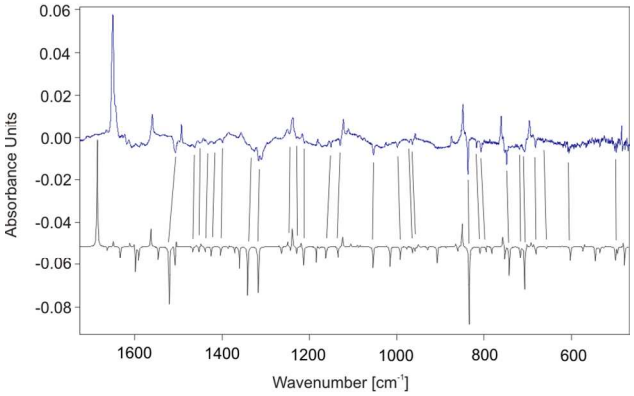

Figure 4. **Top:** Changes in the infrared spectrum of a matrix-isolated sample of **1a** pre-irradiated at 395-nm upon subsequent photolysis at 530 nm; bands belonging to **1a** point up, bands belonging to **4a** point down. **Bottom**: Calculated (B3LYP/6-31G(d), scaled by 0.9614) difference IR spectrum, **1a** – **4a**.

2.3 Oxygen and substituent effects on the formation and decay of 4

Additional confirmation on the nature of the BPQ process was obtained from the study of oxygen and substitution effects on its kinetics. Figure 5 shows the transient absorbance signals obtained upon excitation of **1a-c** in argon- and air-saturated acetonitrile, which are assigned to the formation and decay of **4a-c**. The *p*-OMe derivative **4b** forms and decays faster than the unsubstituted **4a**, (τ_{rise} = 80 ns vs. 160 ns; τ_{decay} = 1.8 μs vs. 8 μs, respectively), consistent with the trends in the production of singlet oxygen, a process competing with BPQ, for two different series of 9-phenyl phenalenone derivatives.[7] Specifically, we found that the quantum yield of singlet oxygen production increases when the electron donating ability of the phenyl substituent decreases. On the other hand, the *o,o'*-dimethyl derivative **4c** forms and decays more slowly (τ_{rise} = 800 ns; τ_{decay} = 12 μs), a clear indication that the steric constraints imposed by the methyl groups control the reaction in this case. Moreover, the strong but incomplete inhibition of the transient signal by oxygen in air-saturated solutions is a clear indication that both the singlet and triplet states can undergo BPQ in all three compounds. This is consistent with previous ultrafast transient absorption data, which showed that the intermediate is formed from the singlet state in 13 ps in acetonitrile.[7]

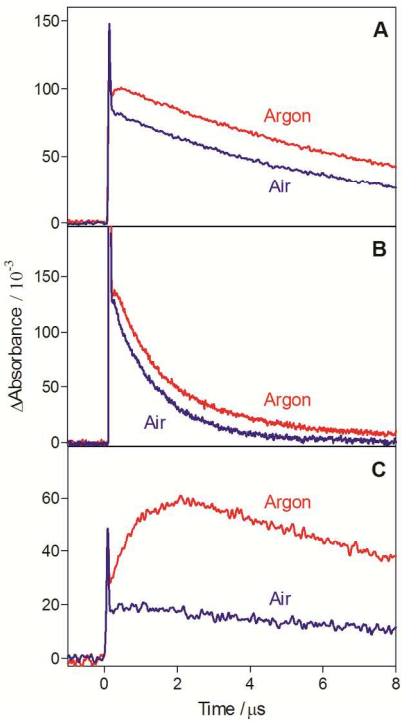

Figure 5: Transient absorption of **1a (A), 1b (B) and 1c (C)** in acetonitrile exciting at 355 nm and observing at 520 nm.

2.4 Reactivity of the BPQ products

At the UM05-2X/6-31G(d) level of theory, the C_{sp3}-H bond in naphthoxanthene **4a** is predicted to be exceedingly weak, with a bond dissociation energy (BDE) of only 28.8 kcal mol^{-1}. This value was arrived at by computing the energies of **4a**, **5a**, and a hydrogen atom, and then calculating the energy difference. It is significantly weaker than the corresponding C-H BDE of phenalene itself, which has been calculated to be 64 kcal mol^{-1}.[20]

The transfer of a hydrogen atom to TCNE, an excellent hydrogen acceptor, would yield naphthoxanthenyl radical **5a** Scheme 3). Alternatively, reaction of **4a** with TCNE could result in a formal hydride transfer (electron and hydrogen atom), leading to the formation of the naphthoxanthenium cation **6a**. Table 1 collects the calculated reaction enthalpies for the two processes in different media.

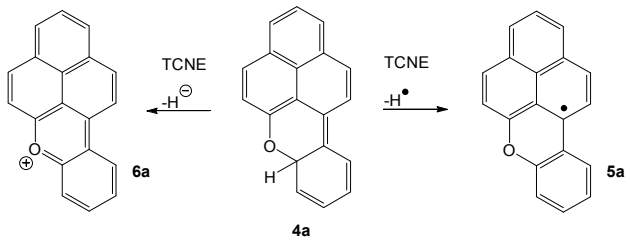

Scheme 3: Reaction pathways upon reaction of 4a with TCNE.

The transition state for hydrogen atom transfer reaction to TCNE has been located (B3LYP/cc-pVTZ//B3LYP/6-

31G(d)). The predicted activation enthalpies is $\Delta H^{\ddagger}$ = 4.9 kcal mol^{-1} relative to separate **4a** and TCNE.

Table 1: Reaction enthalpies for the reactions of 4a with TCNE to yield 5a or 6a, as calculated at the B3LYP/cc-pVTZ//B3LYP/6-31G(d) (gas phase) or (scrf=pcm)- B3LYP/cc-pVTZ//B3LYP/6-31G(d) (solution) levels of theory.[21]

Solvent	ΔH [kcal mol^{-1}] free ions	ΔH [kcal mol^{-1}] free radicals
Vacuum	+29.8	-10.6
Benzene	-14.4	-11.7
Acetonitrile	-46.1	-13.1
Water	-47.5	-13.7

For the reactions of **4a** with TCNE in the gas phase and in acetonitrile solution, we have also calculated intrinsic reaction coordinates. Figure 6A shows a plot of the energy vs. the reaction coordinate. It clearly indicates that the hydrogen transfer reaction is more exothermic in acetonitrile solution, and that it also has an even smaller barrier (ca. 4.5 kcal/mol relative to the **4a**/TCNE complex) in acetonitrile. The geometries of the **4a**/TCNE complex, the TS, and the **5a**/TCNE-H complex are shown in Figure S3 (ESI). The course of the hydrogen transfer reaction is very different in the gas phase and in acetonitrile solution. Figure 6B shows a plot of the Mulliken atomic charge of the hydrogen atom being transferred and of the TCNE moiety vs. reaction coordinate. The hydrogen atom being transferred is an essentially-neutral hydrogen atom both in the gas phase and in acetonitrile solution, i.e., no hydride transfer takes place. Unsurprisingly, the degree of charge transfer is predicted to be much more significant in acetonitrile solution, where already the complex **4a**/TCNE is predicted to largely be a contact ion pair, and where the reaction is predicted to form a full ion pair. Moving along the reaction coordinate, the charge separation is predicted to decrease, reaching a minimum shortly before the transition state. The wavefunctions of the geometries along the reaction coordinate may show significant open-shell character, which is reflected in non-zero calculated Mulliken spin densities. Figure 6C shows a plot of the Mulliken spin densities at carbon atom 34 (which is the central TCNE carbon atom not receiving the hydrogen atom) vs. the reaction coordinate. The data are consistent with a picture in which in acetonitrile, the hydrogen transfer reaction yields a closed-shell ion pair consisting of cation **6a** and the TCNE-H anion, whereas the gas-phase reaction results in formation of a radical pair consisting of **5a** and the TCNE-H radical. In agreement with the analysis of the Mulliken charges, the complex **4a** / TCNE in acetonitrile bears significant spin density at the TCNE moiety, consistent with a description as a **4a**$^{+\cdot}$ / TCNE$^{-\cdot}$ contact ion pair. The overall picture for the hydrogen atom transfer reaction in acetonitrile solution, electron transfer followed by hydrogen atom transfer, agrees with previous findings on similar reactions.[22,23]

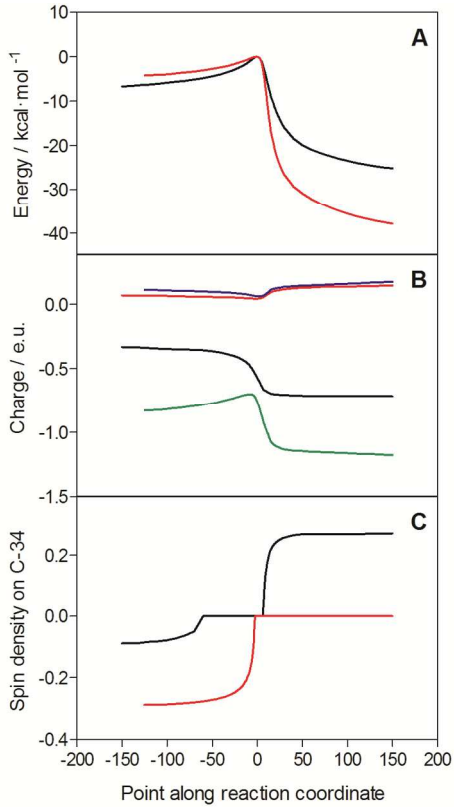

Figure 6: Intrinsic reaction coordinates of the system **4a** + TCNE. The reaction proceeds from left to right, with the transition state at point zero. **A:** Energy, relative to the TS. Black line: gas phase reaction. Red line: solvated by acetonitrile. **B:** Mulliken charges. Red line: charge at migrating hydrogen atom, gas phase. Blue line: charge at migrating hydrogen atom, acetonitrile solution. Black line: charge at TCNE moiety, gas phase. Green line: charge at TCNE moiety, acetonitrile solution. **C:** Mulliken spin density at C-34. Black line: gas phase. Red line: acetonitrile solution.

In the light of the above results, we investigated the products formed in the photolysis of **1a** in the presence of TCNE by UV-Vis, ESR, and ^{1}H-NMR spectroscopies, employing benzene and acetonitrile as solvents. Upon laser (λ = 355 nm) excitation of an argon-saturated **1a** / TCNE solution in benzene, two new bands appeared at λ_{max} = 408 nm and λ_{max} = 460 nm (Figure 7A). When the experiment was conducted in acetonitrile, the 460 nm band dominated at early stages of the photolysis (Figure 7B) and the 408 nm band appeared at later stages (Figure 7C). Deconvolution of the UV/Vis spectra yielded the pure spectra of the two species (Figure 7D), which are in excellent agreement with those of radical **5**a and cation **6**a, obtained independently by chemical synthesis.[8] Consistent with this assignment, the 408 nm species was not observed under an atmosphere of air as one would expect for a carbon-centred radical, whereas the 460-nm band was still present. Prolonging the irradiation, both with laser or with the UV chamber, led to a complex mixture of products. The ESR spectra of the photolysed samples are also consistent with this assignments (see ESI).

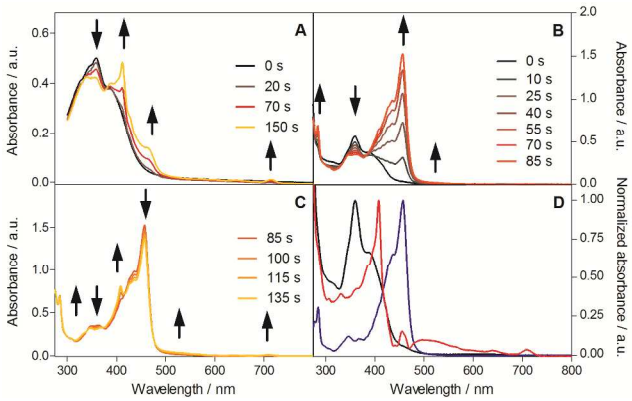

Figure 7: UV-Vis spectral changes upon laser photolysis of **1a** (absorbance 0.5 at 355 nm) in the presence of 150 µM TCNE in argon-saturated solutions. A: In benzene. B: In acetonitrile at early photolysis stages. C: In acetonitrile at later photolysis stages. D: Deconvoluted spectra.

As a final piece of evidence, **1d**, the 9-perdeuterophenyl analogue of **1a** was synthesized and studied by laser flash photolysis and ^{1}H-NMR spectroscopy. While the lifetimes of the two naphthoxanthenes **4a** and **4d** were roughly the same (8 and 7 µs, respectively), the TCNE quenching rate constant for **4d** was 2.3-fold smaller than for **4a** (5.2×10^6 M^{-1} s^{-1} vs. 1.2×10^7 M^{-1} s^{-1}, respectively; Figure 8). The value of the rate constant in benzene was the same as in acetonitrile.

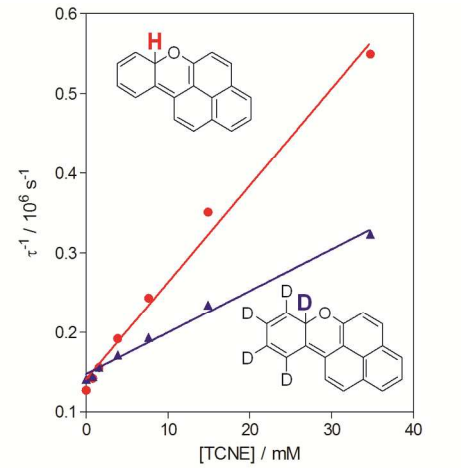

Figure 8: Plot of the reciprocal lifetime of **4a** and **4d** vs. the concentration of TCNE in argon-saturated acetonitrile at room temperature.

The ^{1}H-NMR spectrum of the photolysis products of **1a** and **1d** in argon-saturated acetonitrile in the presence of 5 mM TCNE (Figure 9) are consistent with those of the corresponding naphthoxanthenium cations **6a** and **6d**, respectively.[8] The spectrum of **6d** lacks the signals of four (but not all five) phenyl protons relative to the spectrum of **6a**, which is consistent with a proton having been previously abstracted by TCNE.

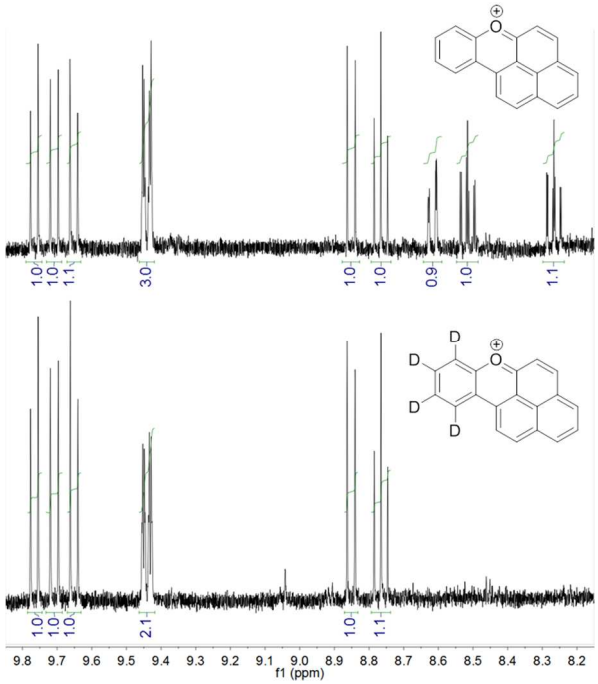

Figure 9: ^{1}H-NMR spectra in acetone-d_6 of **1a** (TOP) and its perdeuterophenyl analogue **1d** (DOWN) after photolysis in the presence of 5 mM TCNE in argon-saturated acetonitrile at room temperature.

2.5 Discussion

The data presented here, including the positive identification of the naphthoxanthene closed-shell product **4a** and of the naphthoxanthenyl radical **5a** and naphthoxanthenium cation **6a** formed upon its reaction with TCNE as well as the kinetic isotope effect on this reaction, strongly advocate for a carbonyl-to-phenyl BPQ addition.[18] The following results are consistent with this interpretation:

1) The experimental UV-Vis and IR spectra of the transient species match those calculated for **4a** (cf. Figures 3 and 4 and ref.[7]). Due to weak absolute intensities, relatively broad IR bands, and band overlap in the difference spectrum, not all IR bands predicted in the calculated IR spectrum can be unequivocally assigned in the experimental spectrum. However, the excellent agreement between calculated and experimental IR band patterns, particularly in the fingerprint region, strongly suggests that the assignment of the red photoproduct to **4a** is correct.

2) There is also an excellent agreement between the calculated and experimental values for the activation enthalpy of the naphthoxanthene **4a** electrocyclic ring opening (7.9-8.9 kcal·mol^{-1} - depending on the calculation method - and 8.8 kcal·mol^{-1}, respectively). Also, the calculations reproduce well the effects of the phenyl substituents.

3) The calculated reactivity of **4a** with TCNE matches the experimental results as well. Specifically, the reaction is predicted to produce the naphthoxanthenyl radical **5a** or the naphthoxanthenium cation **6a** depending on the solvent

polarity (Figure 6), which is unequivocally demonstrated by UV-Vis (Figure 7), and ^{1}H-NMR (Figure 9) spectroscopies. 4) The reaction of **4a** with TCNE shows a strong deuterium isotopic effect (Figure 8), in agreement with expectations for a hydrogen transfer reaction. This is confirmed by comparison of the ^{1}H-NMR data for **6a** and **6d** (Figure 9).

While the results of the current study are in line with the latest insights on BPQ,[18] a number of new aspects to BPQ can be derived. First and foremost, this study shows (Figure 5) that BPQ is not restricted to triplet ketones but applies to their singlet excited states as well, effectively competing with intersystem crossing and therefore with singlet oxygen production.[7] On the other hand, the prediction (Figure 2) and observation of preferential *ortho*-attack in the systems of **1a** and **1b** in is partially due to the rigidity of the phenalenone system and the slightly strained character of the triplet biradicals **3a** and **3b** formed upon *ipso*-attack. Also of importance is probably a stereoelectronic effect: the two π-systems, phenalenone and phenyl, are orthogonal (θ = 180°) in the TS of *ipso*-BPQ of **1a**, whereas the corresponding dihedral is θ = 120° in *ortho*-BPQ (Figure 10). X-Ray data have revealed that the actual dihedral angle is θ = 130 ° [24] thus *ortho* attacks appear more likely.

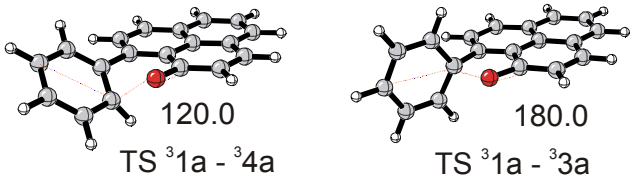

Figure 10: Dihedral angles θ (in °) between the two π-systems in the two TS of BPQ of **1a**

A dihedral θ = 180° would be perfect for BPQ of a (n,π*) triplet excited state, where an unpaired electron is located in a half-filled non-bonding orbital (a former oxygen lone-pair) that lies in the σ-plane of the phenalenone system. Biradical **3a** would therefore correspond with the (n,π*) triplet state of **1a**. For a (π,π*) triplet excited state, where the reactive unpaired electron is located in a π* type antibonding orbital, a parallel orientation of the two π-systems would be ideal. While such a parallel alignment is not accessible due to geometric constraints, a dihedral θ = 130° between the two reaction π-systems means that some (n,π*) character must be acquired along the reaction coordinate. This is completely consistent with the evolution of the spin density at the carbonyl oxygen atom along the reaction coordinates (Figure 2), where *ipso*-BPQ requires a significantly higher spin density at the oxygen atom. It is worth mentioning that phenalenone's lowest triplet state is of (π,π*) character with an upper nπ* triplet state lying only 2.2 kcal·mol^{-1} above.[25] Thus, phenalenone offers a unique scaffold for the control of the BPQ reactivity.

Finally, in the context of the natural occurrence of phenylphenalenones, it is interesting to note that cyclisation products closely related to those described in this work have been isolated from plants (Scheme 4). Indeed, the synthesis of natural naphthoxanthenones (fluorones) from 9-phenylphenalenones, recently proposed to occur by a radical-initiated reaction,[26,27] could also stem from an excited-state cyclisation reaction as described in this report, which suggests a light-mediated metabolic pathway. [28–31] Unravelling the metabolic pathways of phenylphenalenones upon fungal infection of banana plants has recently become of special interest for enhancing their disease resistance to pathogen infection due to the worldwide drop in crops.[32,33]

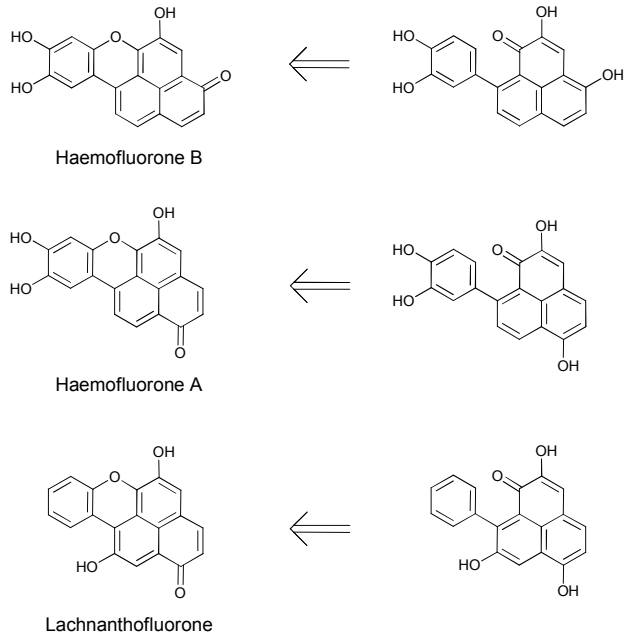

Scheme 4: Possible excited-state pathways for the production of fluorone pigments in plants.

3. Experimental

3.1 Materials

1a-c were synthesized as described elsewhere.[34] Phenalenone and tetracyanoethylene (TCNE) were purchased from Sigma-Aldrich (St Louis, MO) and used as received. Perdeuterobromobenzene was purchased from Cambridge Isotope Laboratories (Andover, MA). All solvents were from Scharlau (Barcelona, Spain), except for deuterated solvents, which were purchased from Sigma-Aldrich (St Louis, MO).

3.2 Computational methods

All calculations were performed using the *Gaussian03* suite of programs.[35] All energy minima and transition structures were fully optimized at the UB3LYP/6-31G(d)[36] level of theory and characterized as such by performing a vibrational analysis. Based on the geometries thus obtained, single point energy calculations were performed at the UB3LYP/cc-pVTZ[37] level of theory. Some of the calculations were repeated using the UB3PW91[36,38] or

UM05-2X[39] hybrid functionals, employing the basis sets mentioned before. Intrinsic reaction coordinate calculations (IRC) were performed starting from the two transition structures relevant to BPQ of **1** and for the transition structures for hydrogen abstraction from **4a** by TCNE (gas phase and solvated by acetonitrile), using broken-symmetry wavefunctions (guess=mix,always) throughout. The reaction coordinates were followed in both directions, using the UB3LYP/6-31G(d) method. Based on the intermediary (nonstationary) geometries thus obtained, again single point energy calculations were performed at the UB3LYP/cc-pVTZ level of theory. The activation and reaction enthalpies given in this work do not include a ZPE correction. The influence of solvation on reaction enthalpies was investigated by performing *Polarizable Continuum Model* (PCM)[40] single point energy calculations at the B3LYP/cc-pVTZ level of theory, based on gas-phase B3LYP/6-31G(d) geometries.

3.3 General spectroscopic measurements

UV/Vis spectra were recorded using a Shimadzu 3600 UV/Vis/NIR spectrometer (Glasgow), a Varian Cary 6000i spectrometer (Barcelona), or a Cary 5000 UV/Vis/NIR spectrometer (Bochum). Irradiation experiments were performed using a Luzchem ORG irradiation chamber equipped with ten UV-A lamps (Glasgow) or a Continuum Surelite II Nd:YAG laser operated at the 3rd harmonic (Barcelona). The pulse energy of the laser was adjusted to 2 mJ / pulse to avoid secondary photochemical reactions. Transient absorption spectra were monitored by nanosecond laser flash photolysis using a Q-switched Nd:YAG Laser (Surelite I-10, Continuum) with right-angle geometry and an analysing beam produced by a Xe lamp (PTI, 75W) in combination with a dual-grating monochromator (mod. 101, PTI) coupled to a UV-Vis radiation detector (PTI 710). The signal was fed to a Lecroy WaveSurfer 454 oscilloscope for digitizing and averaging (typically 10 shots) and finally transferred to a PC computer for data storage and analysis. Matrix isolation experiments were performed using standard matrix isolation equipment.[41] Samples of **1a** were deposited using the slow-spray-on technique, at a sample temperature of $T = 180$ °C.

4. Conclusions

We have shown that excitation of 9-phenylphenalenones **1** results in the formation of the highly reactive naphthoxanthenes **4** by β-phenyl quenching via addition to the *ortho* position of the 9-phenyl substituent. Naphthoxanthene **4a** is highly reactive, undergoing facile electrocyclic ring opening to revert to **1a** in the ground state. It is also an exceedingly potent hydrogen donor, reacting with TCNE to yield the highly-stable naphthoxanthenyl free radical and/or the highly-coloured naphthoxanthenium cation. Photo-induced cyclization in 9-phenylphenalenones is consistent with the natural occurrence of fluorones in plants.

Acknowledgements

R.B.-O. thanks the Generalitat de Catalunya (AGAUR) for a collaboration fellowship. C.F. and S.N. gratefully acknowledge Prof. Jan Verhoeven for helpful discussions and Dr. Lluís Julià for preliminary ESR spectra. G.B. thanks Dirk Grote for the simulation of the ESR spectrum, and Stuart Caldwell for his help in recording it. The research performed in Glasgow is part of the Glasgow Centre for Physical Organic Chemistry funded by the EPSRC. G.B. gratefully acknowledges this funding. A grant from the Spanish Ministry of Science and Innovation is gratefully acknowledged (CTQ2007-67763-C03-01/BQU and CTQ2010-20870-C03-01).
G.B. thanks Wolfram Sander (Ruhr-Universität Bochum, Germany), for providing generous access to matrix isolation equipment.

Notes and references

[a] *WestCHEM, School of Chemistry, University of Glasgow, Joseph-Black-Building, University Avenue, Glasgow G12 8QQ, United Kingdom. e-Mail: goebu@chem.gla.ac.uk*
[b] *Institut Químic de Sarrià, Universitat Ramon Llull, E-08017, Barcelona, Spain. e-Mail: santi.nonell@iqs.url.edu*
[c] *IMDEA Nanociencia, E-28049 Madrid, Spain*
[d] *Instituto Universitario de Bio-Orgánica "Antonio González", Avda. Astrofísico Fco. Sánchez 2, Universidad de La Laguna, E-38206, La Laguna, Tenerife, Canary Islands, Spain*
[e] *Departamento de Química Orgánica, Facultad de Farmacia, Avda. Astrofísico Fco. Sánchez s/n, Universidad de La Laguna, E-38206, La Laguna, Tenerife, Canary Islands, Spain.*

Electronic Supplementary Information (ESI) available: Naturally occurring 9-phenylphenalenones. Synthesis of **1d**. Spin angular momentum vs. C-O distance for *ipso*- and *ortho*-addition in ^{3}**1a***. ESR spectrum of photolysed solutions of **1a** and TCNE. Optimised geometries. See DOI: 10.1039/b000000x/

1. A. Lazzaro, M. Corominas, C. Martí, C. Flors, L. R. Izquierdo, T. A. Grillo, J. G. Luis, and S. Nonell, *Photochem. Photobiol. Sci.*, 2004, **3**, 706–710.
2. C. Flors and S. Nonell, *Acc. Chem. Res.*, 2006, **39**, 293–300.
3. F. Otálvaro, J. Nanclares, L. E. Vásquez, W. Quiñones, F. Echeverri, R. Arango, and B. Schneider, *J. Nat. Prod.*, 2007, **70**, 887–890.
4. E. Oliveros, P. Suardi-Murasecco, T. Aminian-Saghafi, A. M. A. M. Braun, H. Hanseu, and H.-J. Hansen, *Helv. Chim. Acta*, 1991, **74**, 79–90.
5. R. Schmidt, C. Tanielian, R. Dunsbach, and C. Wolff, *J. Photochem. Photobiol. A*, 1994, **79**, 11–17.
6. C. Martí, O. Cuenca, M. Casals, S. Nonell, and O. Jürgens, *J Photochem Photobiol A Chem.*, 1996, **97**, 11– 19.
7. C. Flors, P. R. Ogilby, J. G. Luis, T. a Grillo, L. R. Izquierdo, P.-L. Gentili, L. Bussotti, and S. Nonell, *Photochem. Photobiol.*, 2006, **82**, 95–103.

8. O. Anamimoghadam, M. D. Symes, C. Busche, D.-L. Long, S. T. Caldwell, C. Flors, S. Nonell, L. Cronin, and G. Bucher, *Org. Lett.*, 2013, **15**, 2970–2973.
9. P. J. Wagner, P. A. Kelso, A. E. Kemppainen, A. Haug, and D. R. Graber, *Mol. Photochem.*, 1970, **2**, 81–85.
10. J. C. Scaiano, M. J. Perkins, J. W. Sheppard, M. S. Platz, and R. L. Barcus, *J. Photochem.*, 1983, **21**, 137–147.
11. T. Wismontski-Knittel and T. Kilp, *J. Phys. Chem.*, 1984, **88**, 110–115.
12. J. C. Netto-Ferreira, W. J. Leigh, and J. C. Scaiano, *J. Am. Chem. Soc.*, 1985, **107**, 2617–2622.
13. W. J. Leigh, J.-A. H. Banisch, and M. S. Workentin, *J. Chem. Soc. Chem. Commun.*, 1993, 988–990.
14. J. N. Moorthy, W. S. Patterson, and C. Bohne, *J. Am. Chem. Soc.*, 1997, **119**, 11094–11095.
15. J. N. Moorthy, S. L. Monahan, R. B. Sunoj, J. Chandrasekhar, and C. Bohne, *J. Am. Chem. Soc.*, 1999, **121**, 3093–3103.
16. D. Ng, Z. Yang, and M. A. Garcia-Garibay, *Tetrahedron Lett.*, 2001, **42**, 9113–9116.
17. S. Samanta, B. K. Mishra, T. C. S. Pace, N. Sathyamurthy, C. Bohne, and J. N. Moorthy, *J. Org. Chem.*, 2006, **71**, 4453–4459.
18. G. Bucher, *J. Phys. Chem. A*, 2008, **112**, 5411–5417.
19. A. P. Scott and L. Radom, *J. Phys. Chem.*, 1996, **100**, 16502–16513.
20. S. E. Stein and R. L. Brown, *J. Am. Chem. Soc.*, 1991, **113**, 787–793.
21. B. J. Lynch and D. G. Truhlar, *J. Phys. Chem. A*, 2001, **105**, 2936–2941.
22. S. Fukuzumi, K. Ohkubo, Y. Tokuda, and T. Suenobu, *J. Am. Chem. Soc.*, 2000, **122**, 4286–4294.
23. M. A. Grishina, V. A. Potemkin, and A. I. Matern, *J. Struct. Chem.*, 2008, **49**, 7–12.
24. J. G. Luis, W. Q. Fletcher, F. Echeverri, T. A. Grillo, M. P. Kishi, and A. Perales, *Nat. Prod. Lett.*, 1994, **6**, 23–28.
25. C. Flors and S. Nonell, *J. Photochem. Photobiol. A Chem.*, 2004, **163**, 9–12.
26. L. Duque, C. Restrepo, J. Sáez, J. Gil, B. Schneider, and F. Otálvaro, *Tetrahedron Lett.*, 2010, **51**, 4640–4643.
27. B. Schneider, L. Duque, C. Zapata, and F. Ot, *Org. Lett.*, 2013, **15**, 2011–2014.
28. S. Opitz, D. Hölscher, N. J. Oldham, S. Bartram, and B. Schneider, *J. Nat. Prod.*, 2002, **65**, 1122–1130.
29. J. M. M. Edwards and U. Weiss, *Phytochemistry*, 1974, **13**, 1597–1602.
30. R. Cooke and I. Dagley, *Aust. J. Chem.*, 1979, **32**, 1841–1847.
31. S. Opitz, F. Otálvaro, F. Echeverri, W. Quiñones, and B. Schneider, *Nat. Prod. Lett.*, 2002, **16**, 335–338.
32. D. Butler, *Nature*, 2013, **504**, 195–196.
33. D. Hölscher, S. Dhakshinamoorthy, T. Alexandrov, M. Becker, T. Bretschneider, A. Buerkert, A. C. Crecelius, D. De Waele, A. Elsen, D. G. Heckel, H. Heklau, C. Hertweck, M. Kai, K. Knop, C. Krafft, R. K. Maddula, C. Matthäus, J. Popp, B. Schneider, U. S. Schubert, R. A. Sikora, A. Svatoš, and R. L. Swennen, *Proc. Natl. Acad. Sci. U. S. A.*, 2014, **111**, 105–110.
34. J. G. Luis, W. Q. Fletcher, F. Echeverri, and T. A. Grillo, *Tetrahedron*, 1994, **50**, 10963–10970.
35. M. J. Frisch, et al. *Gaussian03*, Gaussian, Inc., Wallingford CT, 2004
36. A. D. Becke, *J. Chem. Phys.*, 1993, **98**, 5648–5652.
37. R. A. Kendall, T. H. Dunning, and R. J. Harrison, *J. Chem. Phys.*, 1992, **96**, 6796–6806.
38. J. Perdew, K. Burke, and Y. Wang, *Phys. Rev. B*, 1996, **54**, 16533–16539.
39. Y. Zhao, N. E. Schultz, and D. G. Truhlar, *J. Chem. Theory Comput.*, 2006, **2**, 364–382.
40. M. Cossi, G. Scalmani, N. Rega, and V. Barone, *J. Chem. Phys.*, 2002, **117**, 43–54.
41. I. Dunkin, *Matrix Isolation Techniques: A practical approach*, Oxford University Press, Oxford, UK, 1998.